

# First-Principles DFT Insights into the Mechanisms of CO<sub>2</sub> Reduction to CO on Fe (100)-Ni Bimetals

Caroline Kwawu (✉ [kwawucaroline@gmail.com](mailto:kwawucaroline@gmail.com))

Kwame Nkrumah University of Science and Technology <https://orcid.org/0000-0001-5686-1377>

Albert Aniagyei

University of Health and Allied Sciences

Destiny Konadu

Kwame Nkrumah University of Science and Technology

Elliot Menkah

Kwame Nkrumah University of Science and Technology

Richard Tia

Kwame Nkrumah University of Science and Technology

---

## Research Article

**Keywords:** CO<sub>2</sub> decomposition, CO<sub>2</sub> activation, bimetal, Iron alloys, Nickel deposited Surfaces

**Posted Date:** June 24th, 2021

**DOI:** <https://doi.org/10.21203/rs.3.rs-540311/v1>

**License:**  This work is licensed under a Creative Commons Attribution 4.0 International License.

[Read Full License](#)

---

**Version of Record:** A version of this preprint was published at Theoretical Chemistry Accounts on March 1st, 2022. See the published version at <https://doi.org/10.1007/s00214-022-02879-5>.

## **First-Principles DFT Insights into the Mechanisms of CO<sub>2</sub> Reduction to CO on Fe (100)-Ni Bimetals**

Caroline R. Kwawu,<sup>1\*</sup> Albert Aniagyei,<sup>2</sup> Destiny Konadu,<sup>1</sup> Elliot Menkah,<sup>1</sup> Richard Tia<sup>1</sup>

<sup>1</sup>Department of Chemistry, Kwame Nkrumah University of Science and Technology, Kumasi, Ghana

<sup>2</sup>Department of Basic Sciences, University of Health and Allied Sciences, Ho, Ghana

Email: kwawucaroline@gmail.com (C.R.K)

### **Declarations**

### **Funding:**

CRK is grateful for funding from The World Academy of Sciences (grant 18-032 RG/CHE/AF/AC\_I). CRK and RT acknowledges the UK Royal Society and Leverhulme Trust for a research grant under the Royal Society-Leverhulme Africa Postdoctoral Fellowship Award Scheme (grant LAF\R1\180013).

**Conflicts of Interest:** No conflicts of interest

**Availability of data and material:** No additional data available to be shared.

**Code availability:** Quantum Espresso is an opensource code available at <https://www.quantum-espresso.org/>

**Author's contributions:** Data was collected by Mr. Destiny Konadu, Manuscript was drafted by Dr. Caroline Rosemyya Kwawu and revised by Dr. Albert Aniagyei and Dr. Elliot Menkah. Research concept was developed and supervised by Dr. Richard Tia and Dr. Caroline Rosemyya Kwawu.

## Abstract

Iron and nickel are known active sites in the enzyme carbon monoxide dehydrogenases (CODH) which catalyzes  $\text{CO}_2$  to CO reversibly. The presence of nickel impurities in the earth abundant iron surface could provide a more efficient catalyst for  $\text{CO}_2$  degradation into CO, which is a feedstock for hydrocarbon fuel production. In the present study, we have employed spin-polarized dispersion-corrected density functional theory calculations within the generalized gradient approximation to elucidate the active sites on Fe (100)-Ni bimetals. We sort to ascertain the mechanism of  $\text{CO}_2$  dissociation to carbon monoxide on Ni deposited and alloyed surfaces at 0.25, 0.50 and 1 monolayer (ML) impurity concentrations.  $\text{CO}_2$  and (CO + O) bind exothermically i.e., -0.87 eV and -1.51 eV respectively to the bare Fe (100) surface with a decomposition barrier of 0.53 eV. The presence of nickel generally lowers the amount of charge transferred to  $\text{CO}_2$  moiety. Generally, the binding strengths of  $\text{CO}_2$  were reduced on the modified surfaces and the extent of its activation was lowered. The barriers for  $\text{CO}_2$  dissociation increased mainly upon introduction of Ni impurities which is undesired. However, the 0.5 ML deposited (FeNi<sub>0.5</sub>(A)) surface is promising for  $\text{CO}_2$  decomposition, providing a lower energy barrier (of 0.32 eV) than the pristine Fe (100) surface. This active 1-dimensional defective FeNi<sub>0.5</sub>(A) surface provides a stepped surface and Ni-Ni bridge binding site for  $\text{CO}_2$  on Fe (100). Ni-Ni bridge site on Fe (100) is more effective for both  $\text{CO}_2$  binding or sequestration and dissociation compared to the stepped surface providing the Fe-Ni bridge binding site.

**Keywords:**  $\text{CO}_2$  decomposition;  $\text{CO}_2$  activation; bimetals; Iron alloys; Nickel deposited Surfaces

## 1. INTRODUCTION

The levels of carbon dioxide in the atmosphere continues to increase as a result of anthropogenic activities like combustion of fossil fuels, leading to global warming and climate change.[1]  $\text{CO}_2$  is an abundant and cheap carbon-one source, which could be a useful feedstock in the production of transportation fuels,[2] industrial chemicals,[3] and polymers.[1] However, due to the stability and inertness of the  $\text{CO}_2$  molecule, catalysts are required for conversion.[4, 5] Despite difficulties associated with  $\text{CO}_2$  conversion industrially, anaerobic enzymes such as carbon monoxide dehydrogenases are known to reversibly catalyze the reduction of  $\text{CO}_2$  to CO at ambient conditions of temperature and pressure.[6]  $\text{CO}_2$  is said to anchor and receive electrons at the bridge site of iron and nickel in the

Fe-Ni-S cluster in carbon monoxide dehydrogenases.[7] The catalytic CO<sub>2</sub> decomposition into CO has become an active field of research in catalytic chemistry as CO is the feedstock in the Fischer-Tropsch process for the production of long-chain hydrocarbon liquid transportation fuels.[2, 8]

Catalytic conversion of CO<sub>2</sub> to valuable industrial feedstock like CO is an attempt to ease the effects of CO<sub>2</sub> on our environment. Although experimental studies on CO<sub>2</sub> reduction on single crystal surfaces show activity for CO<sub>2</sub> chemisorption and reduction on bare Fe and Ni, including Ni (110) and Fe (111), [9] the energetics and mechanisms of CO<sub>2</sub> transformation to viable products like CO, methane, formic acid etc. on these bare metal surfaces were not well understood. The extent of CO<sub>2</sub> activation and dissociation on iron and nickel surfaces have been shown to be face specific experimentally.[10–14]

This was later supported by other density functional theory (DFT) calculations whereby on iron the barrier to CO<sub>2</sub> dissociation on the low Miller index surfaces were of the trend Fe (100) ~ (111) < (110).[15] Several computational studies have also been carried out to investigate the interactions of CO<sub>2</sub> with Ni, mostly employing the spin-polarized density functional theory-generalized gradient approximation (DFT-GGA) to understand the energetics on their various topologies. [16–24] CO<sub>2</sub> is reported to bind more strongly on iron than nickel while its decomposed species bind stronger to nickel than iron. Kinetically decomposition is observed to be favored on iron than nickel. [21]

Iron and nickel are known active sites in the enzyme carbon monoxide dehydrogenases (CODH) and the presence of nickel impurity in earth-abundant iron could provide more active materials for CO<sub>2</sub> decomposition to CO. CO<sub>2</sub> interactions with bare and 1 ML deposited surfaces of the low Miller index surfaces of iron have been investigated previously,[15] where nickel is seen to alter the ease of CO<sub>2</sub> dissociation. However, to the best of our knowledge, no theoretical studies have been carried out on alloys of iron and nickel and the concentration effect of nickel deposition on the activity of the iron surface has also not been explored. In this present study, we have employed dispersion-corrected spin-polarized-density functional theory calculations within the generalized gradient approximation (DFT-D2-GGA) to elucidate the mechanism of CO<sub>2</sub> reduction into carbon monoxide on the pristine Fe (100) facet, its nickel alloys and nickel deposited surfaces at varying concentrations of 0.25 ML, 0.5 ML and 1 ML.

## 2. COMPUTATIONAL DETAILS

All calculations were carried out with the spin-polarized density functional theory method as implemented in the Quantum ESPRESSO package.[25] The generalized gradient approximation (GGA), with the Perdew, Burke, Ernzerhof (PBE) exchange-correlation functional[26] was used in all simulations. The surface was described by a slab model, where periodic boundary conditions were applied to the central super-cell so that it is reproduced periodically throughout space. XcrysDen [27] software was employed for the visualization of structures and electron densities. The Fermi-surface effects were treated by the smearing technique of Fermi-Dirac, using a smearing parameter of 0.03 Ry. The energy threshold defining self-consistency of the electron density was set to  $10^{-6}$  eV.

Iron (100) surface was cleaved with the METADISE code [28] and a  $p(2 \times 2)$  super-cell was employed for all calculations as the binding energy of CO<sub>2</sub> does not change significantly with increasing super-cell. The slab was built to a thickness of three, made up of six atomic layers. A vacuum of 20 Å was introduced to the surface to prevent interactions between surfaces along the z-axis. The top three layers of the slab was relaxed in all calculations, which has been reported previously to be the converged structure of iron (100).[29] All gaseous adsorbates were optimized in a cubic box of size 20 Å and allowed to relax in all calculations. Neighboring adsorbates in laterally repeating units of the slabs were more than 5 Å apart.

Using convergence tests, the kinetic energy cutoff of the plane wave basis set was set to 40 Ry and 320 Ry for the charge density cut-off. The Monkhorst-pack K-points grid of (7 x 7 x 7), (5 x 5 x 1) and (1 x 1 x 1) were used for bulk, surfaces and adsorbates respectively. The Climbing Image Nudged Elastic Band (CI-NEB) method was used to determine the energy barriers for dissociation. Vibrational modes were calculated whereby a single imaginary frequency was indicative of a transition state. Lowdin charge analysis was employed for charge density characterizations upon adsorption of CO<sub>2</sub>.

### 3. RESULTS AND DISCUSSION

#### 3.1 CO<sub>2</sub> adsorption on Pure and Bimetallic Surfaces

The computation parameters were first validated by calculating the bulk properties of iron. The unit cell of iron crystalizes in the body-centered cubic (BCC) form and our spin-polarized DFT-D2 calculations were able to reproduce the electronic properties of bulk iron.[15, 30]

We considered six different bi-metallic surfaces, i.e., nickel adsorption and absorption as a point defect (P), 1-dimensional defect (1D) and 2-dimensional defect (2D). Hence nickel ad-atom deposition at 3 concentrations i.e., 0.25 ML (FeNi<sub>0.25</sub>(A)), 0.5 ML (FeNi<sub>0.5</sub>(A)) and 1 ML (FeNi<sub>1</sub>(A)), and nickel alloying at 3 concentrations i.e., 0.25ML (FeNi<sub>0.25</sub>(B)), 0.5ML (FeNi<sub>0.5</sub>(B)) and 1-ML (FeNi<sub>1</sub>(B)) (see **Figure 1**). The energetics of bi-metallic surface formation was determined using the defect formation energies below in equation (1);

$$E_{def} = E_{products} - E_{reactants} \quad (1)$$

Equation (1) represents formation energy for the deposition or adding on of ad-atoms and Equation (2) represents formation energy for the doping or replacement of host atoms.

$$E_{def} = \frac{E_{deposited} - (E_{slab} + nE_{Ni})}{n} \quad (2)$$

$$E_{def} = \frac{(E_{doped} + nE_{Fe}) - (E_{slab} + nE_{Ni})}{n} \quad (3)$$

Where  $E_{Fe}$  is energy of single iron atom,  $E_{Ni}$  is energy of single nickel atom,  $n$  is the number of dopants and  $E_{slab}$  is energy of the perfect Fe (100) surface.

**Table 1:** The binding strength of CO<sub>2</sub> ( $E_{ads}$ ), charge gained by CO<sub>2</sub> ( $q$ ), the extent of CO<sub>2</sub> activation ( $C-O_{Avg}$ ) and the Fermi energy ( $E_f$ ) of Ni modified Fe (100) surfaces

Surface	$E_{def}$ / eV	$E_{ads}$ / eV	$q$ / e	C-O <sub>(1)</sub> / Å	C-O <sub>(2)</sub> / Å	C-O <sub>Avg</sub> / Å	$E_f$ / eV
i. Bare Fe	-	-0.87	0.08	1.35	1.36	1.36	3.07

a. FeNi <sub>0.25</sub> (A)	-8.47	-0.33	0.04	1.25	1.25	1.25	2.04
b. FeNi <sub>0.5</sub> (A)	-4.88	-0.47	0.04	1.25	1.25	1.25	2.06
c. FeNi <sub>1</sub> (A)	-5.29	-0.19	0.06	1.30	1.32	1.31	0.90
d. FeNi <sub>0.25</sub> (B)	4.02	-0.92	0.08	1.34	1.35	1.35	2.91
e. FeNi <sub>0.5</sub> (B)	0.53	-0.96	0.08	1.34	1.35	1.35	2.86
f. FeNi <sub>1</sub> (B)	-0.70	-0.84	0.08	1.34	1.35	1.35	2.73

As seen in **Table 1**, deposition is generally favored thermodynamically over alloying, nickel prefers to be segregated on iron than alloy at all concentrations of 0.25 to 1 ML. The high instability of the doped surfaces relative the deposited surfaces show that thermodynamically at 0.25 ML, 0.5 ML and 1 ML concentrations, nickel will be segregated on the surfaces than diffuse to form alloys with the Fe (100) surface. The stability of the Fe-Ni alloys increases with nickel concentration and iron nickel mixing could improve with higher impurity concentrations. The defect formation energies show a stability trend of FeNi<sub>0.25</sub>(B) < FeNi<sub>0.5</sub>(B) < FeNi<sub>1</sub>(B) < FeNi<sub>1</sub>(A) < FeNi<sub>0.5</sub>(A) < FeNi<sub>0.25</sub>(A). The high stability of FeNi<sub>0.25</sub>(A) over FeNi<sub>1</sub>(A) shows that the nickel once on the surface of iron prefers to isolate from neighboring nickel atoms than to coagulate on the surface of iron.

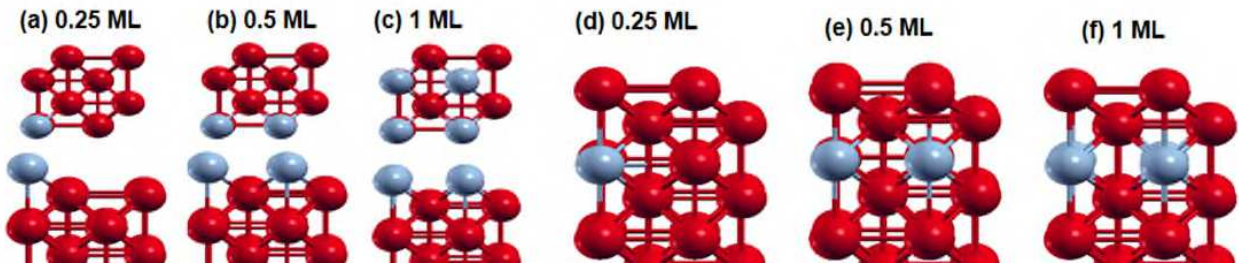


**Figure 1:** Defect formation energies of nickel with iron surfaces, (a) deposition at 0.25 ML, (b) deposition at 0.5 ML, (c) deposition at 1 ML, (d) doping at 0.25 ML, (e) doping at 0.5 ML and (f) doping at 1 ML

Carbon dioxide adsorption was then studied on the pure and defective surfaces (see **Figure 2**) and the binding energies of CO<sub>2</sub> on the various surfaces were calculated as follows;

$$E_{ads} = E(\text{slab} + \text{CO}_2) - (E_{\text{slab}} + E_{\text{CO}_2}) \quad (4)$$

Where  $E_{(\text{slab}+\text{CO}_2)}$  is the energy of the adsorbed system,  $E_{\text{slab}}$  and  $E_{\text{CO}_2}$  are the energies of the isolated surface and gaseous carbon dioxide respectively.

The preferred  $\text{CO}_2$  adsorption site on the clean Fe (100) surface has been reported to be the hollow site in the  $\text{C}_{2v}$  adsorption mode. [15] At the active site i.e., at the hollow site and in the  $\text{C}_{2v}$  preferred  $\text{CO}_2$  adsorption state, we investigated the effect of doping on  $\text{CO}_2$  binding.

As shown in **Figure 3**,  $\text{CO}_2$  binding to bare Fe (100) is exothermic with adsorption energy of -0.87 eV. This is very consistent with earlier observations of -0.9 eV, [15] -0.92 eV,[31] -0.7 eV.[19] Introduction of nickel into the bulk of iron (structure d) at point defect of 0.25 ML, increases the binding strength of  $\text{CO}_2$  to -0.92 eV.  $\text{CO}_2$  coordinates to four iron atoms at the hollow site. Increasing the nickel concentration to 1D defect (structure e) increases the iron- $\text{CO}_2$  interactions at the hollow site to -0.96 eV. While at 2D defect (structure f), the iron- $\text{CO}_2$  interaction at the hollow site is decreased to -0.84 eV, this is less than the binding on bare Fe (100). Comparing the electronegativity of nickel and iron, nickel is more electron withdrawing and increasing its concentration in the bulk of iron, lowers the electron density available at the surface for transfer into the  $\text{CO}_2$  moiety. The nickel electron withdrawing effect is felt at the surface with increasing concentration of nickel. Also increasing the concentration of nickel dopant at the sub-surface site introduces appreciable Ni properties at the surface, as bare Ni is known to bind  $\text{CO}_2$  more weakly. [32]

In Ni adsorption situations as shown in Figure 3a and 3b, stepped surfaces are provided that provide lower surface  $\eta$ - $\text{CO}_2$  coordination and lower binding energies due to the presence of nickel on surfaces compared to the alloyed surfaces in Figure 3d, 3e and 3f. As seen for the nickel single ad-atom at 0.25 ML deposition, the binding takes place at the bridge of iron and nickel, and the strength of binding is weakened to -0.33 eV compared to bare iron. Increasing nickel concentration at the surface decreases the binding strength of  $\text{CO}_2$  further to -0.19 eV for  $(\text{FeNi}_1(\text{B}))$  (c).

Ni generally weakens  $\text{CO}_2$  binding strength except in cases where the Ni effect is less felt on the surface. These results show that decreasing  $\text{CO}_2$  surface coordination by the introduction of adatoms and higher electronegative atom effects like nickel on the surface weakens  $\text{CO}_2$  binding.

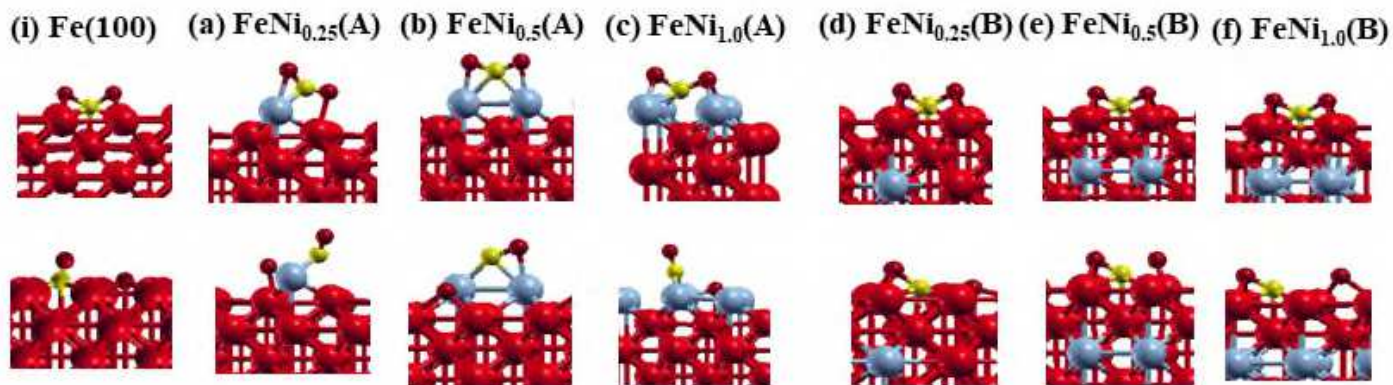


**Figure 2:** CO<sub>2</sub> adsorption on the bare, deposited and doped Fe (100)-Ni surfaces

The net amount of charge gained by CO<sub>2</sub> molecule from the surface and the extent of CO<sub>2</sub> activation on the surfaces has also been characterized and reported in **Table 1**. To understand the factors controlling the CO<sub>2</sub> binding strength and the extent of CO<sub>2</sub> activation various plots were carried out (see **Figure 3**). A plot of CO<sub>2</sub> degree of activation and the amount of charge gained by CO<sub>2</sub> (**Figure 3d**), shows that the more the charge gained by the molecule the more activated the molecule. This is consistent with earlier studies.[23] A regression factor of 0.99 was obtained. A plot of the surface Fermi energy and the amount of charge gained by the CO<sub>2</sub> moiety shows there is no correlation with a regression factor of 0.02. Although the Fermi energy and the charge loss by the surface do not correlate, there is a correlation between the surface Fermi energy and the binding strength of CO<sub>2</sub>. With a regression factor of 0.86 (see **Figure 3c**). Hence Fermi energy does not influence charge transfer and CO<sub>2</sub> degree of activation but influences the binding strength. Generally, Ni impurities reduce the Fermi energy and binding strength of CO<sub>2</sub> to the surfaces. There is however, weak correlation of 0.60 and 0.67 between the binding energy and the variables of CO<sub>2</sub> activation (plot b) and charge gained (plot a) respectively.

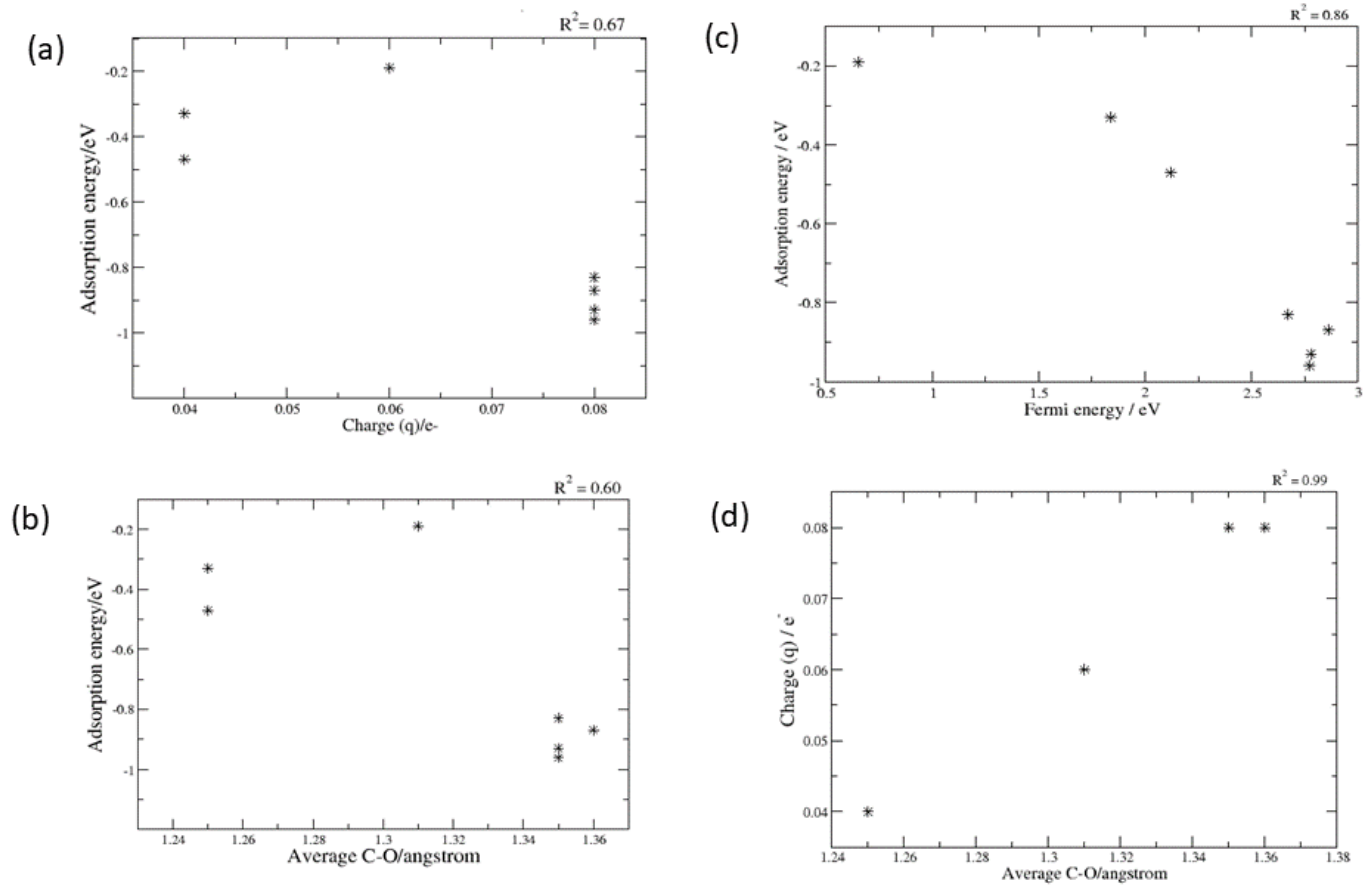


**Figure 3:** Plot of (a) CO<sub>2</sub> binding energy against charge gained by CO<sub>2</sub> molecule (b) CO<sub>2</sub> binding energy against CO<sub>2</sub> extent of activation, (c) CO<sub>2</sub> binding energy against Fermi energy of surface, (d) Charge gained by CO<sub>2</sub> molecule against CO<sub>2</sub> extent of activation

### 3.2 CO<sub>2</sub> Dissociation on Pure and Bimetallic Surfaces

The reaction energies for CO<sub>2</sub> dissociation ( $E_{\text{dis}}$ ) and the barriers for dissociation ( $E_a$ ) were calculated with equation (2) and (3) respectively;

$$E_{\text{dis}} = E_{\text{products}} - (E_{\text{slab}} + E_{\text{CO}_2}) \quad (2)$$

Where  $E_{\text{products}}$  is the energy of the adsorbed dissociated system,  $E_{\text{slab}}$  is the energy of isolated slab and  $E_{\text{CO}_2}$  is the energy of isolated carbon dioxide molecule.

$$E_a = E_{TS} - E_{IS} \quad (2)$$

Where  $E_{TS}$  is energy of the transition state and  $E_{IS}$  is the energy of the intermediate state i.e., adsorbed  $\text{CO}_2$ .

To reduce surface interaction between adsorbed molecules, the decomposed species CO and O were optimized individually on the surfaces as well to determine the binding energies in **Table 2**. As reported in **Table 2**, the binding energy of decomposed  $\text{CO}_2$  ( $E_{\text{dis}}$ ), is generally favorable thermodynamically relative to the binding energy of  $\text{CO}_2$  ( $E_{\text{ads}}$ ). The thermodynamics of the dissociation steps were also calculated relative to the activated  $\text{CO}_2$  moiety ( $\text{Step}_{\text{dis}}$ ) and was found to be a thermodynamically favored step on all surfaces. The reaction barriers for the dissociation steps were then computed for the reactions on the various surfaces. The energy profile diagram showing the energy transitions along the reaction coordinates are shown in **Figure 4**.

**Table 2:** Energies for the adsorption and dissociation reactions as well as energy barriers for each dissociation step

Surface	$\Delta E_{\text{ads}}/ \text{eV}$	$\Delta E_{\text{dis}}/ \text{eV}$	$\text{Step}_{\text{dis}}/ \text{eV}$	$E_a/ \text{eV}$
i. Bare Fe	-0.87	-1.51	-0.64	0.53
a. $\text{FeNi}_{0.25}(\text{A})$	-0.33	-0.83	-0.50	1.97
b. $\text{FeNi}_{0.5}(\text{A})$	-0.47	-0.79	-0.32	0.32
c. $\text{FeNi}_1(\text{A})$	-0.19	-0.52	-0.33	4.16
d. $\text{FeNi}_{0.25}(\text{B})$	-0.92	-2.14	-1.22	0.73
e. $\text{FeNi}_{0.5}(\text{B})$	-0.96	-2.14	-1.18	1.32
f. $\text{FeNi}_1(\text{B})$	-0.84	-1.91	-1.07	1.27

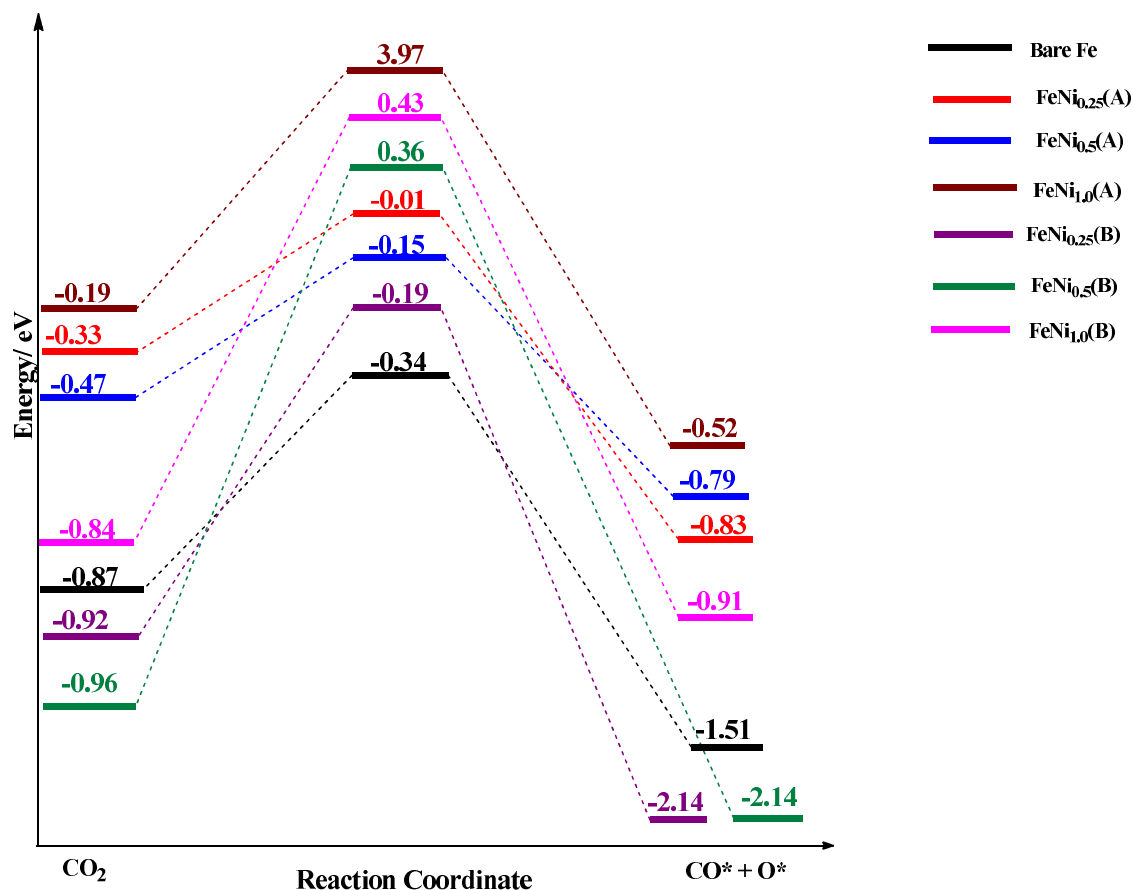


**Figure 4:** Reaction energy profile diagram for CO<sub>2</sub> dissociation on Fe (100) surfaces i.e., pure (Bare Fe), Ni deposited (FeNi<sub>0.25</sub>(A), FeNi<sub>0.5</sub>(A), FeNi<sub>1.0</sub>(A)) and Ni doped (FeNi<sub>0.25</sub>(B), FeNi<sub>0.5</sub>(B), FeNi<sub>1.0</sub>(B)) iron

On bare Fe (100), a dissociation barrier of 0.53 eV was found. Earlier studies reported 0.22 eV[19] and 0.8 eV.[33] Comparing the energy barriers for the CO<sub>2</sub> dissociation step ( $E_a$  in **Table 2**), generally nickel impedes CO<sub>2</sub> dissociation as higher barriers are encountered on the modified surfaces compared to the pure Fe (100) surface. Ease of dissociation is in the order FeNi<sub>0.5</sub>(A) > Fe (100) > FeNi<sub>0.25</sub>(B) > FeNi<sub>1.0</sub>(B) > FeNi<sub>0.5</sub>(B) > FeNi<sub>0.25</sub>(A) > FeNi<sub>1.0</sub>(A). Monolayer deposited (1 ML) FeNi<sub>1.0</sub>(A) surface seems to be the most challenged surface for CO<sub>2</sub> dissociation kinetically, with a barrier of 4.16 eV. This is expected as it is the surface with most nickel atoms and nickel effect on the surface. Here the nickel behaviour is predominating, as nickel surface provide higher decomposition barriers relative to iron.[32] The FeNi<sub>0.5</sub>(A) (1D defect) is promising for CO<sub>2</sub> dissociation kinetically where CO<sub>2</sub> is coordinated at a Ni-Ni bridge site. Although FeNi<sub>0.5</sub>(A) is the least stable of the deposited surfaces, its formation is

thermodynamically favoured and it is also the deposited surface that binds CO<sub>2</sub> the most and is most suitable for CO<sub>2</sub> sequestration.

#### 4. CONCLUSION

The effect of Ni alloying and deposition on the ease of CO<sub>2</sub> direct dissociation has been studied using the DFT method. Nickel prefers to be segregated on iron than alloy at concentration of 0.25 ML up to 1 ML as alloying is seen to be unstable. The stabilities of the modified surfaces were of the order, FeNi<sub>0.25</sub>(B) < FeNi<sub>0.5</sub>(B) < FeNi<sub>1</sub>(B) < FeNi<sub>1</sub>(A) < FeNi<sub>0.5</sub>(A) < FeNi<sub>0.25</sub>(A). CO<sub>2</sub> binds exothermically to bare Fe (100) surface ( $E_{\text{ads}} = -0.87\text{eV}$ ). Ni at the bulk site improves the binding of CO<sub>2</sub> and its applicability for CO<sub>2</sub> sequestration except at 1 ML doping, where the effect of bulk Ni is stronger on the surface. These results show that introduction of high amount of nickel in the bulk of iron weakens CO<sub>2</sub> binding. The Fermi energy of the modified surfaces have a strong correlation to the CO<sub>2</sub> binding strength. Thermodynamically, dissociation is favoured on all surfaces probed. Kinetically, CO<sub>2</sub> dissociation is most favoured on the FeNi<sub>0.5</sub>(A) surface, which is stepped and allows CO<sub>2</sub> to coordinate to two surface Ni atoms. Generally, the barriers for CO<sub>2</sub> dissociation are heightened compared to bare Fe (100), especially on the monolayer deposited (1 ML) FeNi<sub>1</sub>(A) surface. Ni deposition on Fe at 0.5 ML coverage could offer the most viable nickel-modified iron surface for CO<sub>2</sub> reduction and would provide a more reactive surface for CO<sub>2</sub> hydrogen unassisted splitting into CO (a feedstock essential for the Fischer-Tropsch process).

#### 5. ACKNOWLEDGEMENT

C.R.K. is grateful for funding from The World Academy of Sciences (grant 18-032RG/CHE/AF/AC\_I). C.R.K. and R.T acknowledge the UK Royal Society and Leverhulme Trust for a research grant under the Royal Society-Leverhulme Africa Postdoctoral Fellowship Award Scheme (grant LAFR1\180013). The authors acknowledge the Centre for High-Performance Computing (CHPC), South Africa, for additional computing resources.

## REFERENCES

1. Sakakura T, Choi J-C, Yasuda H (2007) Transformation of carbon dioxide. *Chem Rev* 107:2365–87. <https://doi.org/10.1021/cr068357u>
2. Jiang Z, Xiao T, Kuznetsov VL, Edwards PP (2010) Turning carbon dioxide into fuel. *Philos Trans A Math Phys Eng Sci* 368:3343–64. <https://doi.org/10.1098/rsta.2010.0119>
3. Arakawa H, Aresta M, Armor JN, et al (2001) Catalysis research of relevance to carbon management: progress, challenges, and opportunities. *Chem Rev* 101:953–96
4. Solymosi F (1991) The bonding, structure and reactions of CO<sub>2</sub> adsorbed on clean and promoted metal surfaces. *J. Mol. Catal.* 65:337–358
5. Freund H-J, Roberts MW (1996) Surface chemistry of carbon dioxide. *Surf. Sci. Rep.* 25:225–273
6. Wächtershäuser G (1992) Groundworks for an evolutionary biochemistry: the iron-sulphur world. *Prog Biophys Mol Biol* 58:85–201. [https://doi.org/10.1016/0079-6107\(92\)90022-X](https://doi.org/10.1016/0079-6107(92)90022-X)
7. Jeoung J-H, Dobbek H (2007) Carbon dioxide activation at the Ni,Fe-cluster of anaerobic carbon monoxide dehydrogenase. *Science* 318:1461–4. <https://doi.org/10.1126/science.1148481>
8. Schulz H (1999) Short history and present trends of Fischer – Tropsch synthesis. 186:3–12
9. Freund H-J, Behner H, Bartos B, et al (1987) CO<sub>2</sub> adsorption and reaction on Fe(111): An angle resolved photoemission (ARUPS) study. *Surf Sci* 180:550–564. [https://doi.org/10.1016/0039-6028\(87\)90225-1](https://doi.org/10.1016/0039-6028(87)90225-1)
10. Bauer R (1987) Summary Abstract: Face specificity of CO<sub>2</sub> adsorption on iron surfaces. *J Vac Sci Technol A Vacuum, Surfaces, Film* 5:1110. <https://doi.org/10.1116/1.574810>
11. Behner H, Spiess W, Wedler G, Borgmann D (1986) Interaction of carbon dioxide with Fe(110), stepped Fe(100) and Fe(111). *Surf Sci* 175:276–286. [https://doi.org/10.1016/0039-6028\(86\)90236-0](https://doi.org/10.1016/0039-6028(86)90236-0)
12. Yoshida K, Somorjai GA (1978) The chemisorption of CO, CO<sub>2</sub>, C<sub>2</sub>H<sub>2</sub>, C<sub>2</sub>H<sub>4</sub>, H<sub>2</sub> and NH<sub>3</sub> on the clean Fe(100) and (111) crystal surfaces. *Surf Sci* 75:46–60. [https://doi.org/10.1016/0039-6028\(78\)90051-1](https://doi.org/10.1016/0039-6028(78)90051-1)
13. Hess G, Froitzheim H, Baumgartner C (1995) The adsorption and catalytic decomposition of CO<sub>2</sub> on Fe(111) surfaces studied with high resolution EELS. *Surf Sci* 331–333:138–143. [https://doi.org/10.1016/0039-6028\(95\)00177-8](https://doi.org/10.1016/0039-6028(95)00177-8)

14. Nassir MH (1993) Sequential carbon oxygen bond cleavage in chemisorption of CO<sub>2</sub> on Fe(100). *J Vac Sci Technol A Vacuum, Surfaces, Film* 11:2104. <https://doi.org/10.1116/1.578376>
15. Kwawu CR, Tia R, Adei E, et al (2017) CO<sub>2</sub> activation and dissociation on the low miller index surfaces of pure and Ni-coated iron metal: A DFT study. *Phys Chem Chem Phys* 19:19478–19486. <https://doi.org/10.1039/c7cp03466k>
16. Au C, Chen M (1997) A density functional study of CO<sub>2</sub> adsorption on the (100) face of Cu (9, 4, 1) cluster model. *Chem Phys Lett* 4:
17. de la Peña O'Shea V a., González S, Illas F, Fierro JLG (2008) Evidence for spontaneous CO<sub>2</sub> activation on cobalt surfaces. *Chem Phys Lett* 454:262–268. <https://doi.org/10.1016/j.cplett.2008.02.004>
18. Dri C, Peronio A, Vesselli E, et al (2010) Imaging and characterization of activated CO<sub>2</sub> species on Ni(110). *Phys Rev B* 82:165403. <https://doi.org/10.1103/PhysRevB.82.165403>
19. Glezakou V-A, Dang LX, McGrail BP (2009) Spontaneous Activation of CO<sub>2</sub> and Possible Corrosion Pathways on the Low-Index Iron Surface Fe(100). *J Phys Chem C* 113:3691–3696. <https://doi.org/10.1021/jp808296c>
20. Li H-J, Ho J-J (2010) Density Functional Calculations on the Hydrogenation of Carbon Dioxide on Fe(111) and W(111) Surfaces. *J Phys Chem C* 114:1194–1200. <https://doi.org/10.1021/jp909428r>
21. Liu C, Cundari TR, Wilson AK (2012) CO<sub>2</sub> Reduction on Transition Metal (Fe, Co, Ni, and Cu) Surfaces: In Comparison with Homogeneous Catalysis
22. Wang G-C, Jiang L, Morikawa Y, et al (2004) Cluster and periodic DFT calculations of adsorption and activation of CO<sub>2</sub> on the Cu(hkl) surfaces. *Surf Sci* 570:205–217. <https://doi.org/10.1016/j.susc.2004.08.001>
23. Wang S-G, Liao X-Y, Cao D-B, et al (2007) Factors Controlling the Interaction of CO<sub>2</sub> with Transition Metal Surfaces. *J Phys Chem C* 111:16934–16940. <https://doi.org/10.1021/jp074570y>
24. Wang S-G, Cao D-B, Li Y-W, et al (2005) Chemisorption of CO<sub>2</sub> on nickel surfaces. *J Phys Chem B* 109:18956–63. <https://doi.org/10.1021/jp052355g>
25. Giannozzi P, Baroni S, Bonini N, et al (2009) QUANTUM ESPRESSO: a Modular and Open-source Software Project for Quantum Simulations of Materials. *J Phys Condens Matter* 21:395502. <https://doi.org/10.1088/0953-8984/21/39/395502>
26. Perdew JP, Burke K, Ernzerhof M (1996) Generalized Gradient Approximation Made Simple. *Phys Rev Lett* 77:3865–3868. <https://doi.org/10.1103/PhysRevLett.77.3865>

27. Kokalj A (1999) XCrySDen-A New Program for Displaying Crystalline Structures and Electron Densities. *J Mol Graph Model* 17:176–179. [https://doi.org/10.1016/S1093-3263\(99\)00028-5](https://doi.org/10.1016/S1093-3263(99)00028-5)
28. Watson GW, Kelsey ET, de Leeuw NH, et al (1996) Atomistic simulation of dislocations, surfaces and interfaces in MgO. *J. Chem. Soc. Faraday Trans.* 92:433
29. Kwawu CR, Tia R, Adei E, et al (2017) Applied Surface Science Effect of nickel monolayer deposition on the structural and electronic properties of the low miller indices of ( bcc ) iron : A DFT study. *Appl Surf Sci* 400:293–303. <https://doi.org/10.1016/j.apsusc.2016.12.187>
30. Kwawu CR, Tia R, Adei E, et al (2017) Effect of Nickel Monolayer Deposition on the Structural and Electronic Properties of the Low Miller Indices of (bcc) Iron: A DFT Study. *Appl Surf Sci* 400:293–303. <https://doi.org/10.1016/j.apsusc.2016.12.187>
31. Wang H, Nie X, Chen Y, et al (2018) Facet effect on CO<sub>2</sub> adsorption, dissociation and hydrogenation over Fe catalysts: Insight from DFT. *J CO<sub>2</sub> Util.* <https://doi.org/10.1016/j.jcou.2018.05.003>
32. Liu C, Cundari T, Wilson A (2012) CO<sub>2</sub> reduction on transition metal (Fe, Co, Ni, and Cu) surfaces: In comparison with homogeneous catalysis. *J Phys Chem ...* 116 (9):5681–5688
33. Nie X, Meng L, Wang H, et al (2018) DFT insight into the effect of potassium on the adsorption, activation and dissociation of CO<sub>2</sub> over Fe-based catalysts. *Phys Chem Chem Phys.* <https://doi.org/10.1039/c8cp02218f>